Hydroxylation of the eukaryotic ribosomal decoding center affects translational accuracy

Christoph Loenarz[a,1], Rok Sekirnik[a,2], Armin Thalhammer[a,2], Wei Ge[a], Ekaterina Spivakovsky[a], Mukram M. Mackeen[a,b,3], Michael A. McDonough[a], Matthew E. Cockman[c], Benedikt M. Kessler[b], Peter J. Ratcliffe[c], Alexander Wolf[a,4], and Christopher J. Schofield[a,1]

[a]Chemistry Research Laboratory and Oxford Centre for Integrative Systems Biology, University of Oxford, Oxford OX1 3TA, United Kingdom; [b]Target Discovery Institute, University of Oxford, Oxford OX3 7FZ, United Kingdom; and [c]Centre for Cellular and Molecular Physiology, University of Oxford, Oxford OX3 7BN, United Kingdom

Edited by William G. Kaelin, Jr., Harvard Medical School, Boston, MA, and approved January 24, 2014 (received for review July 31, 2013)

The mechanisms by which gene expression is regulated by oxygen are of considerable interest from basic science and therapeutic perspectives. Using mass spectrometric analyses of *Saccharomyces cerevisiae* ribosomes, we found that the amino acid residue in closest proximity to the decoding center, Pro-64 of the 40S subunit ribosomal protein Rps23p (RPS23 Pro-62 in humans) undergoes posttranslational hydroxylation. We identify RPS23 hydroxylases as a highly conserved eukaryotic subfamily of Fe(II) and 2-oxoglutarate dependent oxygenases; their catalytic domain is closely related to transcription factor prolyl *trans*-4-hydroxylases that act as oxygen sensors in the hypoxic response in animals. The RPS23 hydroxylases in *S. cerevisiae* (Tpa1p), *Schizosaccharomyces pombe* and green algae catalyze an unprecedented dihydroxylation modification. This observation contrasts with higher eukaryotes, where RPS23 is monohydroxylated; the human Tpa1p homolog OGFOD1 catalyzes prolyl *trans*-3-hydroxylation. *TPA1* deletion modulates termination efficiency up to ∼10-fold, including of pathophysiologically relevant sequences; we reveal Rps23p hydroxylation as its molecular basis. In contrast to most previously characterized accuracy modulators, including antibiotics and the prion state of the *S. cerevisiae* translation termination factor eRF3, Rps23p hydroxylation can either increase or decrease translational accuracy in a stop codon context-dependent manner. We identify conditions where Rps23p hydroxylation status determines viability as a consequence of nonsense codon suppression. The results reveal a direct link between oxygenase catalysis and the regulation of gene expression at the translational level. They will also aid in the development of small molecules altering translational accuracy for the treatment of genetic diseases linked to nonsense mutations.

translation | hypoxia | ribosomal hydroxylation | 2-oxoglutarate oxygenase | nonsense readthrough

The rises in atmospheric oxygen levels provided life with a new energy source, but necessitated the evolution of regulatory mechanisms (1). Defining how cells regulate protein biosynthesis by the direct addition of oxygen to cellular molecules is of current basic and medicinal interest. Recent work suggests the presence of multiple regulatory levels and interfaces between O_2 and gene expression, many of which are catalyzed by Fe(II)- and 2-oxoglutarate (2OG)-dependent oxygenases, some of which are therapeutic targets (2). The hypoxic response in animals, but not lower organisms, is substantially mediated by prolyl *trans*-4-hydroxylation of the hypoxia-inducible transcription factor (HIF) (3–6). In addition to the gene-specific regulation of transcription via HIF, oxygen-dependent modifications at other interfaces have been discovered: hydroxylation of splicing-related proteins (7), histone lysyl demethylation (8), and 5-methylcytosine hydroxylation (9). In addition to signaling, posttranslational hydroxylations can also have structural roles: prolyl *trans*-4-hydroxylation stabilizes the collagen triple helix, whereas *trans*-3-hydroxylation appears to be destabilizing in collagen (10).

Enzyme-catalyzed hydroxylation of intracellularly localized proteins was once thought to be rare, but accumulating recent evidence suggests it is widespread (11). Motivated by these findings, we investigated whether the translation of mRNA to protein is affected by oxygen-dependent modifications. A rapidly growing eukaryotic cell devotes most of its resources to the transcription, splicing, and transport of ribosomal proteins and rRNA (12). We therefore reasoned that ribosomal modification is a candidate mechanism for the regulation of protein expression.

Here we provide evidence that posttranslational prolyl hydroxylation of ribosomal protein S23 (RPS23) is an evolutionarily conserved modification that regulates translation termination. Mutations to RPS23 and its bacterial homolog (S12) have long been associated with translational accuracy, following from seminal work characterizing *Escherichia coli* growth phenotypes in the presence of the antibiotic streptomycin (13, 14). The finding that S12 mutations that increased or decreased the accuracy of stop codon recognition in *E. coli* had similar effects in yeast suggested

Significance

The processing of DNA sequences into proteins is fine-tuned to meet the conflicting demands of accuracy and speed. DNA mutations can introduce premature stop codons, leading to inactive proteins. We report that oxygen-dependent posttranslational modification of the ribosomal decoding center affects stop codon readthrough in an mRNA sequence-dependent manner. Our work demonstrates that oxygenases catalyzing RPS23 hydroxylation are conserved in eukaryotes, including yeasts, flies, and humans. In basal eukaryotes, RPS23 undergoes two hydroxylations, whereas in animals we only observe one hydroxylation. Yeast ribosomes lacking hydroxylation manifest altered stop codon readthrough up to ∼10-fold. The results reveal oxygen-dependent modifications that regulate translational accuracy and suggest unprecedented approaches to modulating ribosomal accuracy for medicinal application.

Author contributions: C.L. and C.J.S. designed research; C.L., R.S., A.T., W.G., E.S., M.M.M., and A.W. performed research; C.L., R.S., A.T., and A.W. contributed new reagents/analytic tools; C.L., R.S., A.T., W.G., E.S., M.M.M., M.A.M., M.E.C., B.M.K., P.J.R., A.W., and C.J.S. analyzed data; and C.L. and C.J.S. wrote the paper.

The authors declare no conflict of interest.

This article is a PNAS Direct Submission.

Freely available online through the PNAS open access option.

[1]To whom correspondence may be addressed. E-mail: christopher.schofield@chem.ox.ac.uk or christoph.loenarz@chem.ox.ac.uk.

[2]R.S. and A.T. contributed equally to this work.

[3]Present address: School of Chemical Sciences, Faculty of Science and Technology and Institute of Systems Biology, Universiti Kebangsaan Malaysia, Bangi 43600, Malaysia.

[4]Present address: Institute of Molecular Toxicology and Pharmacology, Helmholtz Zentrum München–German Research Center for Environmental Health, 85764 Neuherberg, Germany.

This article contains supporting information online at www.pnas.org/lookup/suppl/doi:10.1073/pnas.1311750111/-/DCSupplemental.

RPS23 serves as a conserved "accuracy center" (15), a proposal later supported by crystallographic analyses (16, 17).

We report that in basal eukaryotes, RPS23 contains an unprecedented dihydroxyprolyl modification, whereas human RPS23 only undergoes a single prolyl *trans*-3-hydroxylation. RPS23 prolyl-3-hydroxylation affects stop codon readthrough in a sequence-specific manner, consistent with the location of the hydroxylation site within the ribosomal decoding center. Small-molecule inhibition of the RPS23 hydroxylases increases production of full-length proteins from sequences containing clinically relevant nonsense mutations, suggesting that ribosome hydroxylation is of therapeutic interest.

Results

Eukaryotic Ribosomes Undergo Posttranslational Hydroxylation. In *Saccharomyces cerevisiae*, hypoxic stress [3% (vol/vol) atmospheric O_2] decreases polysome levels and increases free 40S ribosomal subunits (Fig. S1 *A* and *B*). This effect is exacerbated in severe hypoxia (0.1% O_2; Fig. S1*C*). The only known oxidative modification to the yeast translational machinery is the essential hypusine residue in the eukaryotic translation initiation factor 5A (18); however, this modification does not account for the majority of differences observed in hypoxia (Fig. S1*E*). To investigate whether these differences reflect O_2-dependent modifications, we analyzed ribosomal proteins by intact protein mass spectrometry (MS). We found that a chromatographic peak corresponding to 15,938 Da (±1 Da) is absent in *S. cerevisiae* grown at lower O_2 levels (Fig. 1*A*). In severe hypoxia (0.1% O_2) and near anoxia (1 ppm O_2) peaks with masses 15,922 and 15,906 Da are observed (Fig. 1*B*). Together with immunoreactivity against an RPS23 antibody, these observations identify the modified protein as Rps23p (unmodified calculated 15,906 Da), and imply Rps23p undergoes posttranslational mono- and dihydroxylation modifications (+16 and +32 Da).

Anoxia Affects Translational Accuracy via Tpa1p. Because RPS23 mutations are associated with the modulation of translational accuracy (14, 15), we investigated whether the identified oxidative modifications to Rps23p act similarly, using a dual-luciferase assay measuring readthrough of the yeast bypass of stop codon 4 (*BSC4*) (19) stop codon sequence (Table S1). *Renilla* and Firefly luciferase (Rluc and Fluc) cDNAs are separated by an in-frame stop codon or a sense codon control; their relative ratio allows quantification of stop codon readthrough as a measure of translational accuracy (Fig. S2*A*). Whereas hypoxic (0.1% O_2) *S. cerevisiae* gave similar results to normoxia, translational accuracy significantly increased in an anoxic environment (Fig. 1*C*). Although we were unable to analyze the Rps23p hydroxylation level during reoxygenation due to the low levels of cell mass obtained under anoxic conditions, luciferase assays imply that the effect may be reversible: ~7 h after a shift from anoxia to normoxia, the extent of readthrough returned to that in normoxia.

We investigated whether the Rps23p hydroxylations are enzyme mediated, focusing on 2OG oxygenases because of their roles in animal oxygen sensing (5, 20). Bioinformatic analyses imply there are ~10 *S. cerevisiae* candidate 2OG oxygenases (Fig. S1*F*). Tpa1p is a component of mRNA–protein complexes binding to the mRNA/poly(A) 3′-end, with *TPA1* deletion reported to

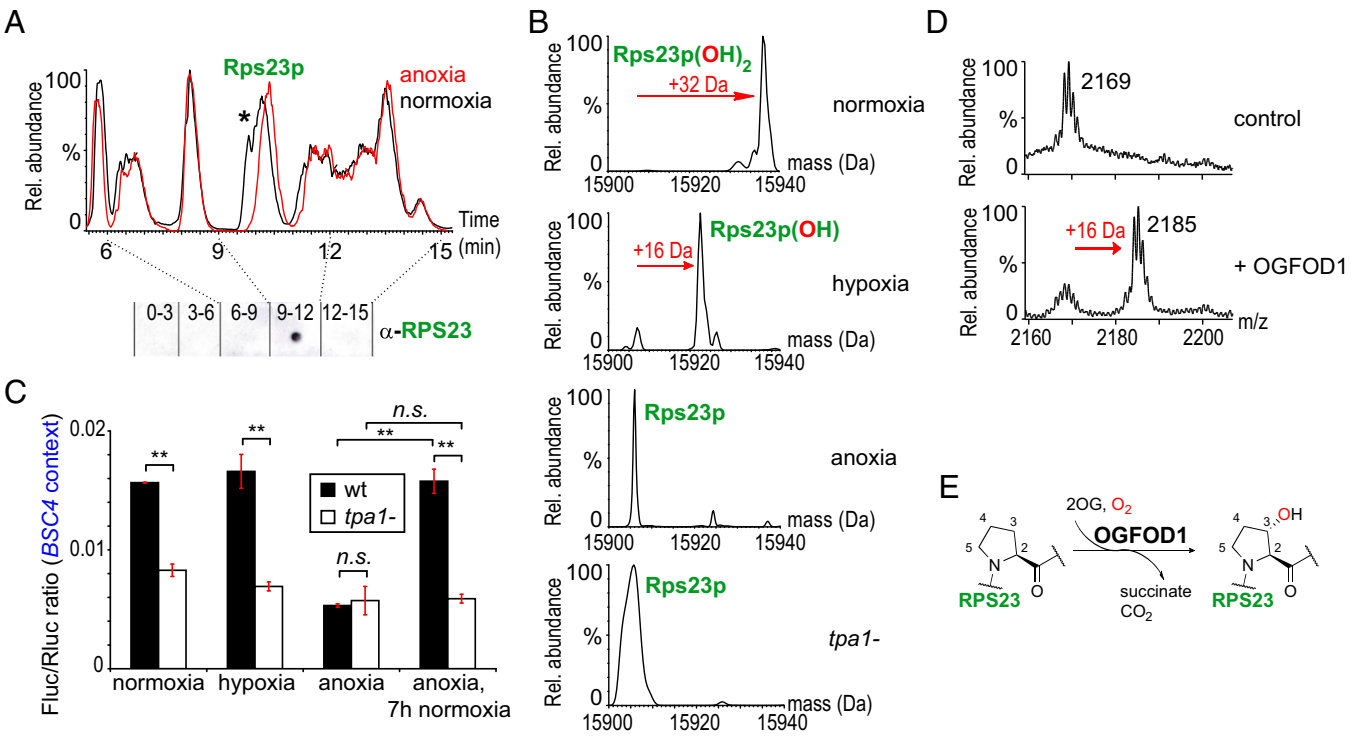

Fig. 1. Tpa1p and its human homolog OGFOD1 catalyze RPS23 prolyl hydroxylation, which affects translational accuracy in yeast. (*A*) UPLC chromatogram of ribosomal proteins from *S. cerevisiae* BY4742 grown in normoxia [21% (vol/vol) O_2] and anoxia (1 ppm O_2). Note the difference in the elution profile: a peak [retention time (R_t) ~9.8 min; highlighted by asterisk] present in normoxia is absent in anoxia. Dot-blot analysis of normoxic UPLC fractions (pooled every 3 min) reveals that fraction 9–12 min cross-reacts with human anti-RPS23 antibody. In anoxia, Rps23p coelutes (R_t ~10.5 min) with Rpl21ap and Rpl21bp (Fig. S7*A*). (*B*) Deconvoluted ribosome ESI-MS spectrum of Rps23p (R_t ~10 min) from *S. cerevisiae* grown in normoxia, hypoxia, and anoxia [21% (vol/vol), 0.1%, and 1 ppm O_2, respectively] and a *tpa1*$^-$ strain. Masses correspond to Rps23p unmodified (15,906 Da, calculated 15,906 Da; N-terminal methionine cleaved) and with addition of one and two oxygen atoms (15,922 Da and 15,938 Da, respectively). (*C*) Effect of changes in O_2 atmosphere [normoxia, 21% (vol/vol) O_2; hypoxia, 0.1% O_2; anoxia, 0.1 ppm O_2] on translational accuracy (Fig. S2*A*) in *S. cerevisiae*. Reoxygenation for 7 h after growth in near-anoxia affects accuracy of WT ($P = 0.003$) but not *tpa1*$^-$ strains ($P = 0.84$). $n = 3$; mean ± SD; $^{**}P < 0.01$; *n.s.*, not significant. (*D*) MALDI MS analyses of $RPS23_{51–70}$ (calculated 2,168.5 Da) after incubation with OGFOD1 and cofactors. (*E*) Reaction scheme showing *trans*-3-hydroxyproline as the catalytic product of OGFOD1-catalyzed hydroxylation of RPS23 Pro-62, as identified by amino acid analysis (Fig. S5).

increase stop codon readthrough (21, 22); however, its substrate was hitherto unknown. Strikingly, the *tpa1*$^-$ strain displays reduced readthrough that was apparently unaffected by O_2 levels and similar to wild-type (WT) levels in anoxia (Fig. 1*C*), suggesting Tpa1p mediates the O_2-dependent pathway that affects translational accuracy. Ribosomal Rps23p from a *tpa1*$^-$ strain lacks oxidative modifications, implying Tpa1p as the Rps23p oxygenase (Fig. 1*B*). Other aspects of translation, including tested frameshifting sites (+1 and −1) and processivity through consecutive rare codons, were unaffected by *TPA1* deletion within limits of detection (Fig. S2 *B–D*). Polysome profiles were unaffected by *TPA1* deletion, suggesting Tpa1p does not directly influence ribosomal biogenesis (Fig. S1*D*).

RPS23 Hydroxylation Conserved Across Eukaryotes. Tpa1p homologs are present in most eukaryotes; they contain an N-terminal 2OG oxygenase domain and a C-terminal double-stranded beta-helix fold (Fig. S3*E*) (22, 23). Consistent with an oxygen-dependent role for Tpa1p in translation, its human homolog 2OG and iron-dependent oxygenase domain containing 1 (OGFOD1) is linked to ischemic signaling/stress responses (24, 25). The Tpa1p homolog in *Schizosaccharomyces pombe* (Ofd1) regulates transcription in a hypoxia-dependent manner via the sterol-responsive transcription factor Sre1 (not present in *S. cerevisiae*) (26, 27); although proposed as a prolyl-4-hydroxylase, no Ofd1 catalytic activity has been described.

As described in the companion articles (28, 29), human OGFOD1 and fruit fly Sudestada1 also catalyze RPS23 oxidation, but result in monohydroxylation of Pro-62. To investigate the evolution of oxidative RPS23 modifications, we prepared Tpa1p/OGFOD1/Ofd1 homologs including from the green algae *Ostreococcus tauri* (otOGFOD1) and fission yeast (Ofd1) as purified proteins. All Tpa1p homologs display catalytic activity with purified GST-$RPS23_{44–143}$ protein, as demonstrated by 2OG turnover (Fig. S4 *D* and *E*). However, to date we have observed that only purified human OGFOD1 catalyzes hydroxylation of $RPS23_{51–70}$ peptide fragments in a 2OG oxygenase characteristic manner; alanine-scanning analyses are consistent with monohydroxylation at Pro-62 (Fig. 1*D* and Fig. S4 *A–C*). Unexpectedly, and in contrast to HIFα prolyl *trans*-4-hydroxylation (5), amino acid analyses using synthetic standards identify *trans*-3-hydroxyproline as the OGFOD1 product (Fig. 1*E* and Fig. S5).

Using coexpression studies of Tpa1p homologs and RPS23 in *E. coli* coupled with proteomic tandem MS, we identify RPS23 Pro-62 (Pro-64 in yeast Rps23p; Fig. S3*D*) as the conserved site of oxidative modifications (Fig. 2*A* and Fig. S6). Human OGFOD1 and fruit fly Sudestada1 were found to catalyze Pro-62 monohydroxylation [companion articles (28, 29)], whereas Tpa1p, Ofd1, and otOGFOD1 produce a mass increment corresponding to a dihydroxyproline residue (Fig. S6). Dihydroxyproline is an unusual amino acid, previously identified as a component of diatom cell walls and *Amanita* mushroom toxin peptides, but

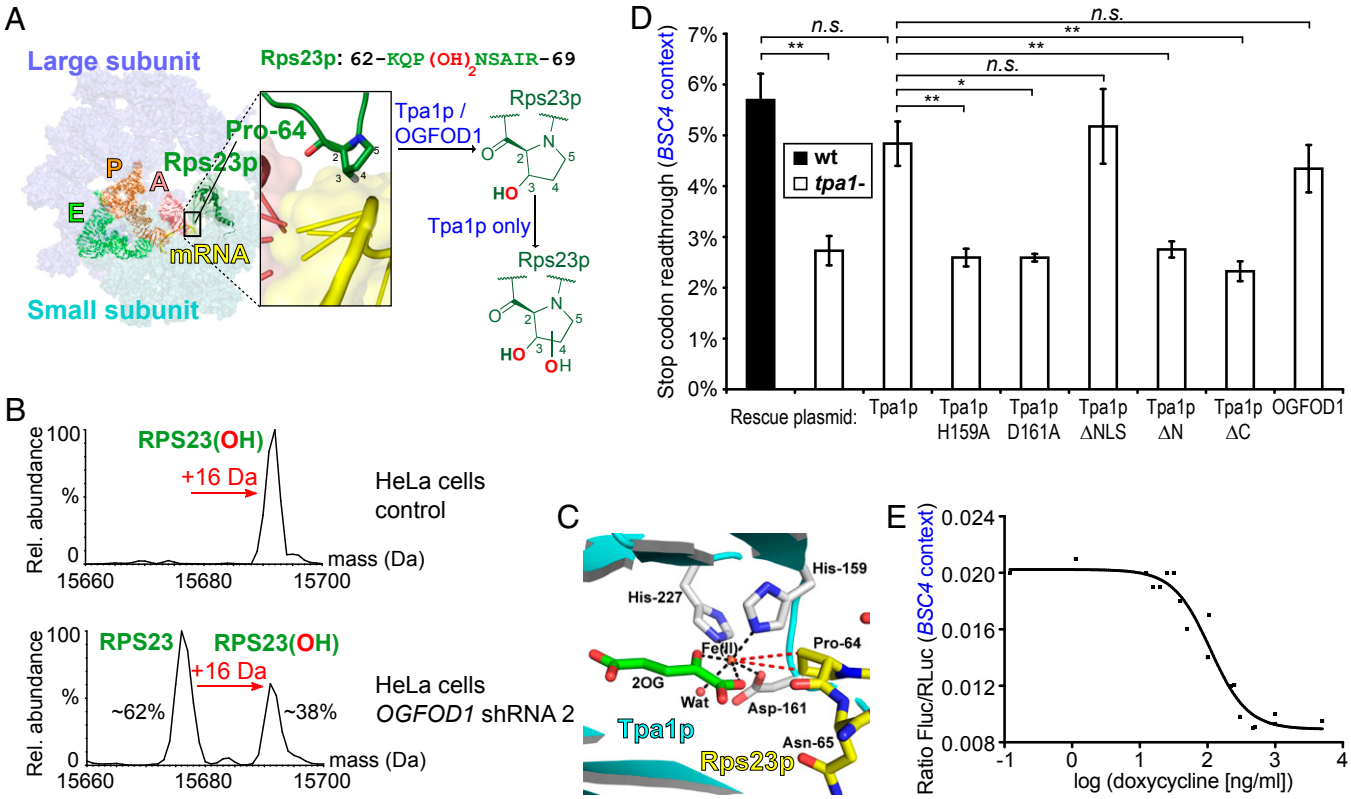

Fig. 2. OGFOD1 and Tpa1p catalyze RPS23 *trans*-3-hydroxyprolyl and dihydroxyprolyl formation, respectively. (*A*) Schematic depicting Tpa1p/OGFOD1 hydroxylation near the ribosomal decoding center; Rps23p Pro-64 is located at the apex of a loop protruding from a β-strand. View of a structure of the bacterial 70S ribosome including tRNAs and mRNA (yellow), with Rps23p (forest green) modeled onto bacterial S12 [Protein Data Bank (PDB) ID codes 2J00, 2J01, and 3U5C] (17, 30). (*B*) Deconvoluted ESI-MS spectrum of RPS23 after UPLC-separation of ribosomes from HeLa cells stably transfected with doxycycline-inducible *OGFOD1* shRNA 2. Observed masses in control (15,692 Da) and induced (15,676 Da) cells correspond to monohydroxylated and unmodified RPS23 (calculated 15,676 Da; N-terminal methionine cleaved), respectively. (*C*) View of the Tpa1p active site (cyan/gray; PDB ID code 3KT7) (22) with ribosomal Rps23p (yellow; PDB ID code 3U5C) (30) modeled into the active site (Fig. S3*C*). Wat, water. (*D*) Reduced *BSC4* stop codon readthrough from *TPA1* deletion ($P = 0.003$) is rescued by a Tpa1p plasmid ($P = 0.095$). Tpa1p Fe(II) binding (H159A, D161A) and domain deletion (ΔN, ΔC) variants are inactive ($P = 0.006$, 0.011, 0.008, and 0.004, respectively), whereas Tpa1p ΔNLS ($P = 0.54$) and OGFOD1 ($P = 0.25$) are similar to WT Tpa1p. $n = 3$; mean ± SD; $^*P < 0.05$; $^{**}P < 0.01$; *n.s.*, not significant. (*E*) A doxycycline-repressible *TPA1* plasmid affects *BSC4* stop codon readthrough in a *tpa1*$^-$ strain (IC_{50} = 110.1 ± 1.2 ng/mL doxycycline; 95% confidence interval 76.1–159.2 ng/mL; $R^2 = 0.9573$; values are pooled from $n = 2$).

which has not previously been identified in intracellular proteins (30, 31). Given the chemically stable nature of the dihydroxylated RPS23 product, the identification of the OGFOD1 product as a *trans*-3-hydroxyproline residue, and a model of ribosomal (32) Rps23p complexed with Tpa1p (22) (Fig. 2*C* and Fig. S3*C*), we propose a 3,4-dihydroxyproline residue as the likely product of two Tpa1p, Ofd1, or otOGFOD1 catalytic cycles.

Consistent with the in vitro studies, ribosomal RPS23 from *S. pombe* (Fig. S7*C*) and *Drosophila melanogaster* S2 cells [companion article (29)] undergoes di- and monohydroxylation, respectively. MS analysis of intact ribosomal proteins in HeLa cells reveals monohydroxylation without evidence of dihydroxylation (Fig. 2*B*). These results suggest that the second RPS23 hydroxylation identified in simpler eukaryotes is not evolutionarily conserved in the tested animals. To investigate whether OGFOD1 catalyzes RPS23 monohydroxylation in cells, we reduced OGFOD1 levels to ∼5% of control using shRNA (Fig. S3 *A* and *B*); ribosomal RPS23 monohydroxylation decreased substantially (to ∼40% of normal levels; Fig. 2*B*).

Rps23p Prolyl *Trans*-3-Hydroxylation Affects Translation Termination in Yeast. To investigate differences between mono-/dihydroxylation, we rescued *S. cerevisiae tpa1*$^-$ strains with *OGFOD1* or *TPA1*; ribosomal Rps23p was monohydroxylated (+16 Da) by human OGFOD1 demonstrating that mono- or dihydroxylation product selectivity is not a consequence of different cellular contexts (Fig. S7*B*). Whereas the Tpa1p nuclear localization sequence (NLS) is not required for Rps23p dihydroxylation, inactivating variants of its iron-binding site (D161A) and domain deletion (ΔN, ΔC) variants ablate Rps23p hydroxylation. Readthrough assays reveal that whereas *tpa1*$^-$ rescue with Tpa1p or OGFOD1 restores WT accuracy levels, variants (H159A and D161A) that disrupt Fe(II) binding have no effect (Fig. 2*D*). Tpa1p ΔNLS, but not its ΔN or ΔC variants, restore WT accuracy levels. A dose–response relationship of Tpa1p levels on accuracy was identified using doxycycline-repressible *TPA1* rescue; at intermediate doxycycline levels, ribosomal Rps23p was present in unmodified, mono- and dihydroxylated forms (Fig. 2*E* and Fig. S7*B*). The combined results imply that prolyl *trans*-3-hydroxylation exerts the major effect on accuracy whereas the second hydroxylation, observed in some eukaryotes, does not play a substantial role, at least for the tested stop codon context.

Biological Relevance of Rps23p Hydroxylations. To investigate the molecular consequences of Rps23p hydroxylation, we undertook comparisons with known modulators of translational accuracy. The prion state of the *S. cerevisiae* translation termination factor 3 (eRF3), termed "[*PSI*$^+$]" cells (33), reduces termination efficiency with benefits for survival (34, 35), but does not affect ribosomal Rps23p hydroxylation (Fig. S7*B*). *TPA1* deletion in [*PSI*$^+$] cells also decreases readthrough of the *BSC4* stop codon, suggesting the role of Tpa1p is independent of eRF3 levels (Fig. 3*A*). Consistent with a critical role for the structure of the Rps23p Pro-64 loop in translation (Fig. 3*B*), N65P and all tested Pro-64 variants are lethal; some substitutions at nearby residues affect growth (Fig. S8 *A*–*C*). As observed in yeast and prokaryotes (13–15), Rps23p Lys-62 variants have opposing effects: K62T is hyperaccurate (approximately fivefold), whereas K62R substitution decreases accuracy approximately ninefold (Fig. S8*D*).

In some yeast strains, a nonsense stop codon in an adenine biosynthesis gene (ADEnine-requiring; *ADE1*) causes red pigmentation; this pigmentation is reduced under conditions that decrease accuracy via nonsense suppression, providing an alternative assay for termination efficiency (36). Notably, *TPA1* deletion ablates red pigmentation, which is rescued by WT but not inactive Tpa1p (Fig. 3*C*). Further, *tpa1*$^-$ but not WT yeast grows on medium lacking adenine (Fig. 3*D*). Together, these results suggest that Rps23p hydroxylation decreases *ADE1* readthrough, but increases readthrough of *BSC4* (the initial context of our luciferase reporters). Consistent with the pigmentation observations, luciferase reporter-measured *ADE1* readthrough significantly

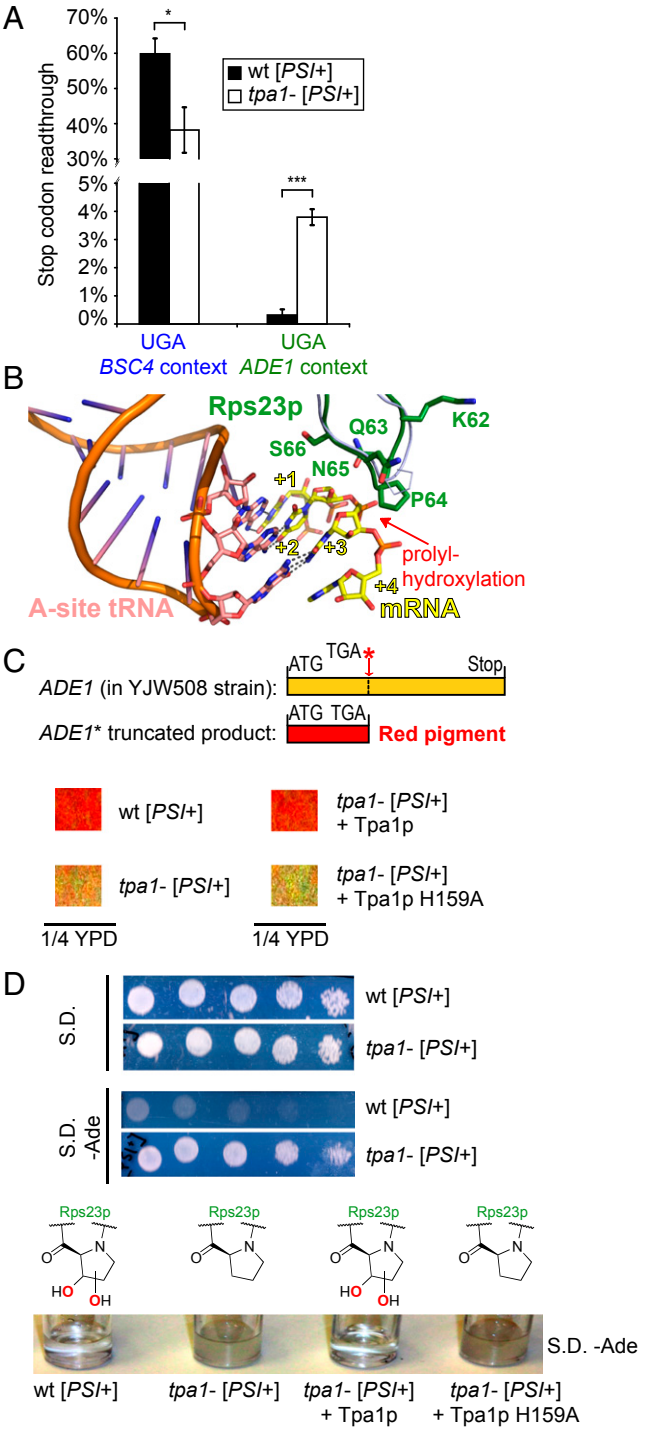

Fig. 3. Physiological relevance of altered stop codon readthrough via Rps23p hydroxylation. (*A*) *TPA1* deletion affects readthrough of the *BSC4* and *ADE1* stop codons ($P = 0.012$ and 0.00013, respectively) ($n = 3$; mean ± SD; $*P < 0.05$; $***P < 0.001$; *y* axis interrupted for clarity). (*B*) View of the decoding site of the bacterial ribosome (17) with Rps23p (30) (green) modeled onto prokaryotic S12 (light-blue ribbon) (PDB ID codes 2J00, 2J01, and 3U5C). Integers indicate mRNA (yellow) codon positions. (*C*) *TPA1* deletion leads to loss of red pigmentation as a consequence of increased readthrough of an *ADE1* nonsense codon present in the YJW508 strain; this effect is reversed by plasmid rescue with WT Tpa1p but not an inactive variant (H159A). Views from suspension cultures in diluted yeast extract peptone dextrose (YPD) medium (Fig. S8*E*). (*D*) *tpa1*$^-$ but not WT YJW508 strains grow in medium lacking adenine both on agar (*Upper*; fivefold serial dilutions) and in suspension (*Lower*); an effect that is reversed by plasmid rescue with WT but not inactive (H159A) Tpa1p.

increases ~10-fold upon *TPA1* deletion (Fig. 3*A*). The directional effect of Rps23p hydroxylation on accuracy is independent of stop codon identity (UGA, UAA, and UAG) for both *BSC4* and *ADE1* contexts (Fig. S2 *E* and *F*). These results imply that Tpa1p regulates accuracy in a sequence-/context-dependent and biologically relevant manner.

Relevance to Clinical Nonsense Mutations. In contrast to the finding that Rps23p hydroxylation increases *BSC4* but decreases *ADE1* readthrough, other modulating factors consistently either increase (Rps23p K62T) or decrease (Rps23p K62R, reduced eRF3 levels, paromomycin) accuracy independent of context (Fig. 4*A*). We therefore analyzed additional stop codon contexts, including from Tobacco mosaic virus (TMV) and nonsense codons of medicinal interest (Fig. S2*G*). Nonsense suppression of *Mdx* from the Duchenne muscular dystrophy mouse model increases upon *TPA1* deletion, an effect that was mirrored by WT cells grown with a cell-penetrating Tpa1p inhibitor (Fig. 4*B*), suggesting that inhibition of RPS23 hydroxylation may be of therapeutic interest (37).

Sequence alignments suggest that the identity of the first nucleotide after the stop codon (+4) may contribute to the directional effect of Rps23p hydroxylation (Fig. 4*C*); statistically, the +4 nucleotide is the least random within mammalian termination contexts (38), and can significantly affect translation termination (39, 40). Structural analyses of Rps23p predict that the Pro-64 *trans*-3-hydroxyl group introduced by Tpa1p/OGFOD1 catalysis is positioned to interact in the ribosomal A site with the phosphate backbone between the third base of the mRNA triplet codon and that in the +4 position (Fig. 3*B*). Importantly, substituting the +4 nucleotide from C to A (or A to C) inverts the directionality of accuracy modulation by Tpa1p for several tested contexts (Fig. 4*D*), i.e., *TPA1* deletion decreases readthrough of the *ADE1* UGAC and TMV UAGC stop codon but increases *ADE1* UGAA and TMV UAGA readthrough. Thus, Rps23p hydroxylation modulates the mRNA–ribosome chemical microenvironment, in a manner relevant to translational accuracy.

Discussion

Overall, given the roles of 2OG oxygenases in transcription factor, chromatin, and DNA hydroxylation/demethylation (3, 4, 7–9, 20), there is accumulating evidence that 2OG oxygenases contribute to an integrated and context-dependent regulation of gene expression. The finding that OGFOD1/Tpa1p catalysis can regulate the accuracy of translation via termination efficiency in an mRNA sequence-dependent manner opens up a unique interface between oxygenase catalysis and the regulation of protein biosynthesis. One possibility is that OGFOD1/Tpa1p catalysis is involved in regulating the translation of specific sets of mRNA sequences, including those involved in the hypoxic response, although at present it is unclear whether ribosome hydroxylation plays a direct role in cellular oxygen sensing. It is possible that ribosomal oxygenase-catalyzed modifications in animals, including those to RPL27A and RPL8 that we recently identified (41), as well as to tRNAs (42–44), help to regulate the sets of genes upregulated by hypoxia in a context-dependent manner. In the two companion articles (28, 29), we provide evidence that Tpa1p catalyzed Rps23p hydroxylation is conserved in humans and fruit flies, and that it is of physiological importance.

The observation that a small posttranslational modification, i.e., addition of a single oxygen atom, can either increase or decrease translational accuracy, is unprecedented. We also note that RPS23 hydroxylation occurs in close proximity to the binding site of known antibiotics, including streptomycin and paromomycin, offering prospects for the targeting of hypoxic tissue via selective inhibition of unhydroxylated RPS23.

Materials and Methods

Luciferase Assay Measurements. Cells from liquid cultures of *S. cerevisiae* strains grown to OD_{600} 0.4–0.6 were lysed for 25 s using Passive Lysis Buffer (all reagents from Promega Dual-Luciferase Reporter Assay System). Fluc activity was measured (10-s integration time) using reconstituted Luciferase Assay Buffer in a GloMax 20/20 luminometer (Promega). Rluc activity (10-s integration time) was determined subsequent to quenching of Fluc activity using Stop & Glo Buffer. Signals were >10-fold above background. The Fluc:Rluc activity ratio is reported. To account for potential differences in translational processivity, the percentage stop codon readthrough of a strain was determined as the ratio of Fluc:Rluc signals of a stop codon bearing insert to that of a sense codon control.

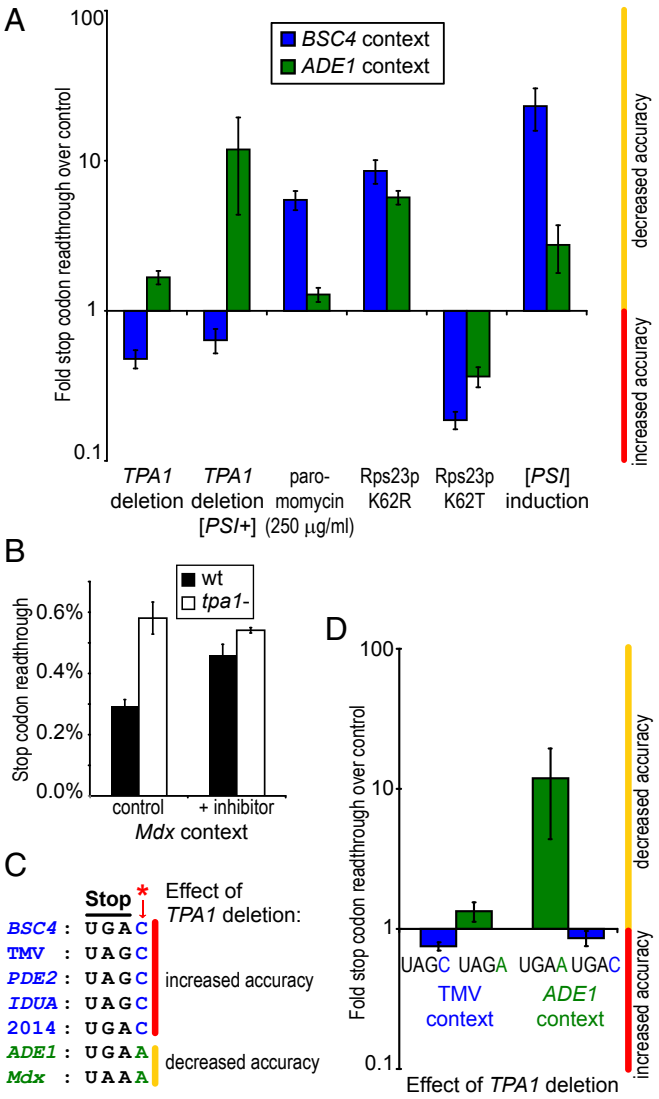

Fig. 4. Effect of Rps23p hydroxylation on translation termination is sensitive to mRNA sequence context. (*A*) Whereas the directional effect of known accuracy modulators is sequence independent, *TPA1* deletion reduces *BSC4* but increases *ADE1* readthrough ($n = 3$; mean ± SD; logarithmic *y* axis). Relative ratios refer to controls [WT BY4742, except for *TPA1* deletion [*PSI*$^+$] (WT [*PSI*$^+$] YJW508) and *PSI* induction (WT [*psi*$^-$] YJW508)]. (*B*) The generic 2OG oxygenase inhibitor dimethyloxalylglycine (10 mM) increases readthrough of the *Mdx* stop codon in WT but not *tpa1*$^-$ BY4742 strains ($n = 2$; mean ± SD). (*C*) Sequence alignment of tested stop codon contexts depicting the directional effect of Rps23p hydroxylation on readthrough (Fig. S2*G*). (*D*) Swapping of the +4 nucleotide within TMV and *ADE1* termination sequences inverts the directional effect of *TPA1* deletion on readthrough in BY4742 and YJW508 [*PSI*$^+$] strains, respectively. Relative ratios refer to WT controls ($n = 3$; mean ± SD; logarithmic *y* axis).

Hypoxic and Anaerobic Cell Growth. Hypoxic culture growth was performed in an Invivo$_2$ Hypoxic Workstation (Ruskinn Life Sciences) at 30 °C, attached to a Ruskinn gas mixer module. Near-anoxic growth was performed in an anaerobic glove box (Belle Technology UK Ltd.) at 18 °C. All media, starter

cultures, growth flasks, and cell-harvesting equipment were preequilibrated at the desired O_2 concentration for 2–4 d. Cell lysis was performed in the presence of 10 mM pyridine-2,4-dicarboxylic acid (Sigma) to inhibit oxygenase activity.

Ribosomal Ultraperformance Liquid Chromatography–Electrospray Ionization Time-of-Flight MS. Samples of purified ribosomal proteins were analyzed by reversed-phase–ultraperformance liquid chromatography (RP-UPLC) and electrospray ionization time-of-flight MS (ESI-TOF MS). The method uses an Acquity UPLC BEH, C4 RP column (2.1 × 50 mm, 1.7-μm particle size, 300-Å pore size; Waters Ltd.). A flow rate of 0.3 mL/min was used with the column held at 50 °C using a Waters Acquity UPLC system connected directly to an LCT ESI-TOF MS (Waters Ltd.). The column was equilibrated with solvent A [0.2% formic acid (HCOOH) in H_2O]. Typically, 5 μL ribosomal protein sample was injected onto the column and proteins eluted using a stepped gradient from solvent A to solvent B (0.1% HCOOH in acetonitrile). The following MS parameters were used: polarity, ES^+; capillary voltage, 3,000 V; sample cone voltage, 35 V; extraction cone voltage, 2.5 V; desolvation temperature, 250 °C; cone gas flow, 10 L/h; and desolvation gas flow (N_2), 500 L/h. The mass spectra were acquired from 400 to 2,400 *m/z* using MassLynx 4.1 software (Waters Ltd.) and protein spectra deconvoluted using Maxent 1 with a range 5–30 kDa (1-Da resolution). Masses were confirmed using manual component analysis. Sodium formate was used as the external calibrant for the instrument. Leucine enkephalin was used as the lock-mass calibrant for internal calibration of samples.

Cell Culture for *OGFOD1* shRNA Knockdown Experiments. For lentiviral transduction, subconfluent cells were incubated with lentiviral stock for 24 h before puromycin selection (1–5 μg/mL). Clonal selection was performed by the dilution series of puromycin-resistant cell populations, until formation of distinct colonies could be observed. All work involving doxycycline-inducible lentivirus was conducted in medium containing high-quality Tet system-approved FBS (Clontech) to avoid fortuitous induction of shRNA expression. Induction of shRNA used 1.5 μg/mL doxycycline every 2 d. Primary antibodies were polyclonal rabbit anti-OGFOD1 (1:500; HPA003215; Sigma-Aldrich), rat HRP-anti–beta-actin (1:25,000; ab49900 [AC-15]; Abcam), and mouse anti-RPS23 (1:1,000; MCA3433Z; AbD Serotec). Secondary antibodies were goat HRP–anti-rabbit (1:500; 170–6515; Bio-Rad Immun-star) and goat HRP–anti-mouse (1:100,000; A9917; Sigma-Aldrich).

Statistical Analyses. For dual-luciferase assays, the probability (*P* values) that two populations are the same was tested using Student *t* test (two-tailed; assuming groups have unequal variance).

ACKNOWLEDGMENTS. We thank Jonathan S. Weissman for the YJW508 strain, Jean-Pierre Rousset for the pAC99 vector, Bastiaan Evers for inducible shRNA vectors, Jamie Cate for the pRS425 plasmid, Hervé Moreau for *O. tauri* genomic DNA, Matthias W. Hentze and Andreas E. Kulozik for the pCI–Renilla plasmid, and Matthew C. Whitby for the MCW1221 strain. We also thank Rachelle S. Singleton and Pablo Wappner for discussions, Joanna F. McGouran for data analysis, and Peter Sharratt for amino acid analyses. C.L. acknowledges a Leverhulme Trust Early Career Fellowship and a Junior Research Fellowship at St. Edmund Hall (University of Oxford). We thank Cancer Research UK (to R.S. and A.T.) and the Slovenian Academy for Sciences and Arts (to R.S.) for studentships. A.W. was a recipient of a European Molecular Biology Organization long-term fellowship. We also thank the Biotechnology and Biological Sciences Research Council UK, the Wellcome Trust, and the European Research Council for funding our work.

1. Holland HD (2006) The oxygenation of the atmosphere and oceans. *Philos Trans R Soc Lond B Biol Sci* 361(1470):903–915.
2. Loenarz C, Schofield CJ (2011) Physiological and biochemical aspects of hydroxylations and demethylations catalyzed by human 2-oxoglutarate oxygenases. *Trends Biochem Sci* 36(1):7–18.
3. Jaakkola P, et al. (2001) Targeting of HIF-alpha to the von Hippel-Lindau ubiquitylation complex by O2-regulated prolyl hydroxylation. *Science* 292(5516):468–472.
4. Ivan M, et al. (2001) HIFalpha targeted for VHL-mediated destruction by proline hydroxylation: Implications for O2 sensing. *Science* 292(5516):464–468.
5. Schofield CJ, Ratcliffe PJ (2004) Oxygen sensing by HIF hydroxylases. *Nat Rev Mol Cell Biol* 5(5):343–354.
6. Loenarz C, et al. (2011) The hypoxia-inducible transcription factor pathway regulates oxygen sensing in the simplest animal, Trichoplax adhaerens. *EMBO Rep* 12(1):63–70.
7. Webby CJ, et al. (2009) Jmjd6 catalyses lysyl-hydroxylation of U2AF65, a protein associated with RNA splicing. *Science* 325(5936):90–93.
8. Tsukada Y, et al. (2006) Histone demethylation by a family of JmjC domain-containing proteins. *Nature* 439(7078):811–816.
9. Tahiliani M, et al. (2009) Conversion of 5-methylcytosine to 5-hydroxymethylcytosine in mammalian DNA by MLL partner TET1. *Science* 324(5929):930–935.
10. Myllyharju J, Kivirikko KI (2004) Collagens, modifying enzymes and their mutations in humans, flies and worms. *Trends Genet* 20(1):33–43.
11. Cockman ME, Webb JD, Kramer HB, Kessler BM, Ratcliffe PJ (2009) Proteomics-based identification of novel factor inhibiting hypoxia-inducible factor (FIH) substrates indicates widespread asparaginyl hydroxylation of ankyrin repeat domain-containing proteins. *Mol Cell Proteomics* 8(3):535–546.
12. Warner JR (1999) The economics of ribosome biosynthesis in yeast. *Trends Biochem Sci* 24(11):437–440.
13. Gorini L, Kataja E (1964) Streptomycin-induced oversuppression in *E. coli*. *Proc Natl Acad Sci USA* 51:995–1001.
14. Triman KL (2007) Mutational analysis of the ribosome. *Adv Genet* 58:89–119.
15. Alksne LE, Anthony RA, Liebman SW, Warner JR (1993) An accuracy center in the ribosome conserved over 2 billion years. *Proc Natl Acad Sci USA* 90(20):9538–9541.
16. Carter AP, et al. (2000) Functional insights from the structure of the 30S ribosomal subunit and its interactions with antibiotics. *Nature* 407(6802):340–348.
17. Selmer M, et al. (2006) Structure of the 70S ribosome complexed with mRNA and tRNA. *Science* 313(5795):1935–1942.
18. Schnier J, Schwelberger HG, Smit-McBride Z, Kang HA, Hershey JW (1991) Translation initiation factor 5A and its hypusine modification are essential for cell viability in the yeast Saccharomyces cerevisiae. *Mol Cell Biol* 11(6):3105–3114.
19. Namy O, et al. (2003) Identification of stop codon readthrough genes in Saccharomyces cerevisiae. *Nucleic Acids Res* 31(9):2289–2296.
20. Loenarz C, Schofield CJ (2008) Expanding chemical biology of 2-oxoglutarate oxygenases. *Nat Chem Biol* 4(3):152–156.
21. Keeling KM, Salas-Marco J, Osherovich LZ, Bedwell DM (2006) Tpa1p is part of an mRNP complex that influences translation termination, mRNA deadenylation, and mRNA turnover in Saccharomyces cerevisiae. *Mol Cell Biol* 26(14):5237–5248.
22. Kim HS, et al. (2010) Crystal structure of Tpa1 from Saccharomyces cerevisiae, a component of the messenger ribonucleoprotein complex. *Nucleic Acids Res* 38(6):2099–2110.
23. Henri J, et al. (2010) Structural and functional insights into Saccharomyces cerevisiae Tpa1, a putative prolylhydroxylase influencing translation termination and transcription. *J Biol Chem* 285(40):30767–30778.
24. Wehner KA, Schütz S, Sarnow P (2010) OGFOD1, a novel modulator of eukaryotic translation initiation factor 2alpha phosphorylation and the cellular response to stress. *Mol Cell Biol* 30(8):2006–2016.
25. Saito K, Adachi N, Koyama H, Matsushita M (2010) OGFOD1, a member of the 2-oxoglutarate and iron dependent dioxygenase family, functions in ischemic signaling. *FEBS Lett* 584(15):3340–3347.
26. Hughes BT, Espenshade PJ (2008) Oxygen-regulated degradation of fission yeast SREBP by Ofd1, a prolyl hydroxylase family member. *EMBO J* 27(10):1491–1501.
27. Lee CY, Yeh TL, Hughes BT, Espenshade PJ (2011) Regulation of the Sre1 hypoxic transcription factor by oxygen-dependent control of DNA binding. *Mol Cell* 44(2):225–234.
28. Singleton RS, et al. (2014) OGFOD1 catalyzes prolyl hydroxylation of RPS23 and is involved in translation control and stress granule formation. *Proc Natl Acad Sci USA* 111:4031–4036.
29. Katz MJ, et al. (2014) *Drosophila* ribosomal prolyl-hydroxylase required for mRNA translation, cell homeostasis and organ growth. *Proc Natl Acad Sci USA* 111:4025–4030.
30. Buku A, Faulstich H, Wieland T, Dabrowski J (1980) 2,3-trans-3,4-trans-3,4-Dihydroxy-L-proline: An amino acid in toxic peptides of Amanita virosa mushrooms. *Proc Natl Acad Sci USA* 77(5):2370–2371.
31. Nakajima T, Volcani BE (1969) 3,4-dihydroxyproline: A new amino acid in diatom cell walls. *Science* 164(3886):1400–1401.
32. Ben-Shem A, et al. (2011) The structure of the eukaryotic ribosome at 3.0 Å resolution. *Science* 334(6062):1524–1529.
33. Osherovich LZ, Weissman JS (2001) Multiple Gln/Asn-rich prion domains confer susceptibility to induction of the yeast [PSI(+)] prion. *Cell* 106(2):183–194.
34. Patino MM, Liu JJ, Glover JR, Lindquist S (1996) Support for the prion hypothesis for inheritance of a phenotypic trait in yeast. *Science* 273(5275):622–626.
35. True HL, Berlin I, Lindquist SL (2004) Epigenetic regulation of translation reveals hidden genetic variation to produce complex traits. *Nature* 431(7005):184–187.
36. True HL, Lindquist SL (2000) A yeast prion provides a mechanism for genetic variation and phenotypic diversity. *Nature* 407(6803):477–483.
37. Linde L, Kerem B (2008) Introducing sense into nonsense in treatments of human genetic diseases. *Trends Genet* 24(11):552–563.
38. McCaughan KK, Brown CM, Dalphin ME, Berry MJ, Tate WP (1995) Translational termination efficiency in mammals is influenced by the base following the stop codon. *Proc Natl Acad Sci USA* 92(12):5431–5435.
39. Namy O, Hatin I, Rousset JP (2001) Impact of the six nucleotides downstream of the stop codon on translation termination. *EMBO Rep* 2(9):787–793.
40. Bonetti B, Fu L, Moon J, Bedwell DM (1995) The efficiency of translation termination is determined by a synergistic interplay between upstream and downstream sequences in Saccharomyces cerevisiae. *J Mol Biol* 251(3):334–345.
41. Ge W, et al. (2012) Oxygenase-catalyzed ribosome hydroxylation occurs in prokaryotes and humans. *Nat Chem Biol* 8(12):960–962.
42. Fu Y, et al. (2010) The AlkB domain of mammalian ABH8 catalyzes hydroxylation of 5-methoxycarbonylmethyluridine at the wobble position of tRNA. *Angew Chem Int Ed Engl* 49(47):8885–8888.
43. Noma A, et al. (2010) Expanding role of the jumonji C domain as an RNA hydroxylase. *J Biol Chem* 285(45):34503–34507.
44. van den Born E, et al. (2011) ALKBH8-mediated formation of a novel diastereomeric pair of wobble nucleosides in mammalian tRNA. *Nat Commun* 2:172.